Mater. Res. Soc. Symp. Proc. Vol. 845 © 2005 Materials Research Society AA1.6

Biodegradable Microfluidic Scaffolds for Vascular Tissue Engineering

C. J. Bettinger[1,3], J. T. Borenstein[3], R. S. Langer[2]

[1]Department of Materials Science and Engineering, MIT
[2]Department of Chemical Engineering, MIT
Room E25-342
Cambridge, MA, 02139

[3]Charles Stark Draper Laboratory
555 Technology Square
Cambridge, MA, 02139

Abstract

This work describes the integration of novel microfabrication techniques for vascular tissue engineering applications in the context of a novel biodegradable elastomer. The field of tissue engineering and organ regeneration has been borne out of the high demand for organ transplants. However, one of the critical limitations in regeneration of vital organs is the lack of an intrinsic blood supply. This work expands on the development of scaffolds for vascular tissue engineering applications by employing microfabrication techniques. Unlike previous efforts, this work focuses on fabricating single layer and three-dimensional scaffolds from poly(glycerol-sebacate) (PGS), a novel biodegradable elastomer with superior mechanical properties. The transport properties of oxygen and carbon dioxide in PGS were measured through a series of time-lag diffusion experiments. The results of these measurements were used to calculate a characteristic length scale for oxygen diffusion limits in solid PGS scaffolds. Single layer and three-dimensional microfluidic scaffolds were then produced using fabrication techniques specific for PGS. This work has resulted in the fabrication of solid PGS-based scaffolds with biomimetic fluid flow and capillary channels on the order of 10 microns in width. Fabrication of complex, three-dimensional microfluidic PGS scaffolds was also demonstrated by stacking and bonding multiple microfluidic layers.

Introduction

Overcoming the problems of nutrient transport is critical in the design of tissue engineering scaffolds that are targeted for the growth of complex organs such as the liver and kidney. One approach to solving this problem involves the integration of an intrinsic vascular network within these scaffolds. More specifically, the application of microfabrication and BioMEMS technology has been focused toward developing microfluidic networks with geometries that simulate vascular networks[1,2]. Microfabrication is an attractive tool for vascular tissue engineering because of the ability to produce structures with feature resolution of less than 10 microns, the same approximate dimensions of the smallest capillaries. However, one limiting factor in previous studies of microfluidic scaffolds has been the choice of material. Microfabricated silicon and replica molded poly(dimethyl siloxane) (PDMS), although ubiquitous and inexpensive, are not biodegradable, have limited biocompatibility, and therefore are not suitable biomaterials for a tissue engineering scaffold. Microfluidic scaffolds fabricated

from poly(L-lactic-glycolic acid) have poor mechanical properties, undesirable degradation kinetics, and questionable biocompatibility.

Poly(glycerol-sebacate) (PGS), a recently synthesized biocompatible and biodegradable elastomer with superior mechanical properties, serves as a promising alternative material for fabricating microfluidic vascular scaffolds[3]. PGS is a tough, biodegradable, elastomer that is biocompatible, inexpensive, and easy to synthesize. Sebacic acid and glycerol, the monomers used in PGS synthesis, are found naturally in the body and have been FDA approved, respectively. Both *in vitro* and *in vivo* biocompatibility studies [3,4] suggest improved cellular response and morphology of PGS when compared to PLGA. Perhaps the most suitable characteristic of PGS in terms of fabricating scaffolds is the "tunability" of the properties depending upon the curing conditions that are used to prepare the thermoset polymer. For example, simply curing PGS for a shorter period of time can produce relatively adhesive polymer films. These adhesive layers could then be strongly bonded to other PGS layers by bringing them into contact and subsequently curing them again thereby forming a chemical bond between the layers. This ability to fabricate individual PGS polymer layers independently and the bond them together is of critical importance when fabricating microfluidic scaffolds.

This investigation integrates microfabrication techniques with the novel biomaterial PGS to synthesize microfluidic scaffolds that are suitable for vascular tissue engineering. By combining unique biomaterials with microfluidics, unprecedented control of the cellular microenvironment can be achieved. Furthermore, these microenvironments can be manipulated in ways to elicit desirable cellular responses to eventually organize into complex tissues and organs.

Experimental Method

Transport Properties of Oxygen and Carbon Dioxide Gas in PGS Membranes. It is desirable for tissue engineering systems to be able to freely transport oxygen and carbon dioxide. Therefore, the initial thrust of this study focused on elucidating the relevant transport properties of oxygen and carbon dioxide (permeability (P), solubility (S), and diffusivity (D)) through a series of simple-time lag diffusion experiments. PGS membranes were synthesized by curing PGS pre-polymer[3] into flat sheets. The membrane was placed in a diffusion chamber and evacuated for at least 120 hrs by applying vacuum to both sides across the membrane. After the evacuation procedure had finished, a sample gas or either oxygen or carbon dioxide was supplied at a pressure of 1 atm to the topside of the membrane as the pressure was continuously measured on the downside. Each experiment produced a time evolution of pressure, which was used to calculate the solubility, diffusivity, and permeability[5].

Fabrication of Microfluidic PGS Scaffolds. Standard photolithographic and plasma etching techniques were utilized to produce "negative mold" silicon masters for use in replica molding just as PDMS is used to fabricate microfluidic devices quickly and easily[6]. Various mask layouts (Figure 1) were designed to achieve different microfluidic geometries. The height of the silicon features varied from 35 microns to 100 microns depending on the type of layer with uniformities of +/- 1%. Molds for first-generation vascular layers, second-generation vascular layers, and parenchymal layers had feature heights of 35, 50, and 100 microns, respectively. Prior to replica molding of PGS, a sacrificial sucrose release layer was spin-coated on the silicon master. PGS

pre-polymer was melted at 160°C and applied to the top-side of the wafers for replica molding and unpatterned sheet formation. Two curing recipes were used to obtain two variations of PGS with different properties. The first curing recipe baked the polymer at 150°C for 15 hours under a vacuum of 20 mTorr, which produced firm, highly cross-linked PGS layers. The second curing recipe baked the polymer at 130°C for 18 hours under 20 mTorr of vacuum, which produced a more deformable PGS layer that is partially crosslinked. The highly crosslinked patterned PGS layer can be affixed to an unpatterned partially crosslinked layer to form the microfluidic device (Figure 2). Once the layers are assembled and sandwiched together, the devices are cured in a final bonding process. Prior to this final curing step, vertically oriented inlet and outlet ports were made by punching out 1/8" OD holes in the highly crosslinked layer in both the single and multi-layered devices. Two types of multi-layered devices were fabricated; coupled flow and decoupled (independent) flow. Coupled flow devices contained one set of inlet/outlet ports where one type of liquid at a given flow rate was pumped in parallel into all the stacked microfluidic layers. Independent flow devices contained multiple sets of inlet/outlet ports where multiple liquids could be pumped through different microfluidic layers at various flow rates. These different devices were fabricated by varying the orientation of individual microfluidic layers, the locations of the inlet/outlet ports, and the vertical thru-hole connections between each microfluidic layer. Once the final curing step was completed, silicone tubing (1/16" ID, 1/8" OD, Cole-Parmer) was inserted into the devices in a sterile environment. Luer-Lok connections were inserted into the tubing and the base of the connections was sealed with epoxy (McMaster-Carr).

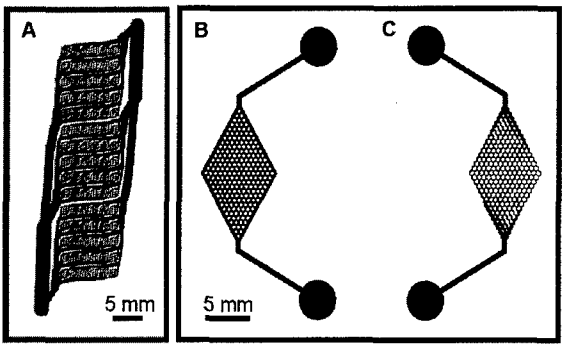

Figure 1. Mask Layout for Silicon Masters. Feature heights of 35, 100, and 50 microns were used in the fabrication of networks A, B, and C respectively. A) A first-generation vascular bed was designed to simulate the scaling of the reduction in the sizes from arterioles to capillaries. B-C) Second-generation masks of a parenchymal and vascular layers, respectively, for use in three-dimensional devices.

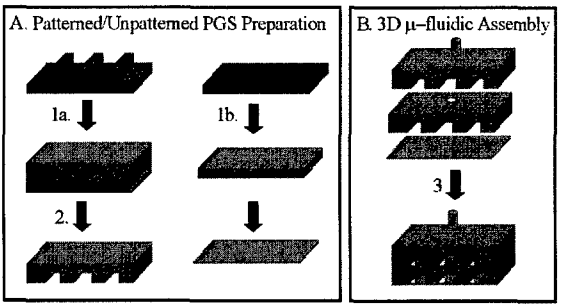

Figure 2. PGS Microfluidic Fabrication. A) Micromachined and blank silicon wafers are used for the preparation of patterned and blank PGS sheets respectively. After melting the PGS pre-polymer on the respective substrate, the polymer is cured and delaminated from the wafer. B) Inlet/outlet ports were integrated in the top layer of the device and subsequent thru holes were made into the intermediate layers of the coupled-flow device. The layers were then bonded to form the final device.

Results

Transport Coefficients of Carbon Oxygen and Carbon Dioxide Gas in PGS Membranes. A summary of the results is shown in Table 1. The steady state flux of the gas is characterized by the value of the permeability (P), which was used to calculate the characteristic length scale for diffusion in solid PGS tissue engineering scaffolds.

Table 1. Summary of Transport Coefficients of Oxygen and Carbon Dioxide in PGS @ 25°C.

	Coefficient	Sample Size, N	Average, $\bar{X}$	Standard Deviation, σ	σ (%)
Oxygen	**P** x 10^{17} (m^3 STP-m)/(m^2-sec-N/m^2)	7	6.23	0.788	34.1
	D x 10^{12} (m^2/sec)	7	3.42	1.17	12.6
	S x 10^{5} (m^3 STP)/(m^3-N/m^2)	7	2.03	0.792	39.0
Carbon Dioxide	**P** x 10^{17} (m^3 STP-m)/(m^2-sec-N/m^2)	3	13.6	3.44	22.8
	D x 10^{12} (m^2/sec)	3	2.15	0.490	25.3
	S x 10^{5} (m^3 STP)/(m^3-N/m^2)	3	6.30	0.260	4.13

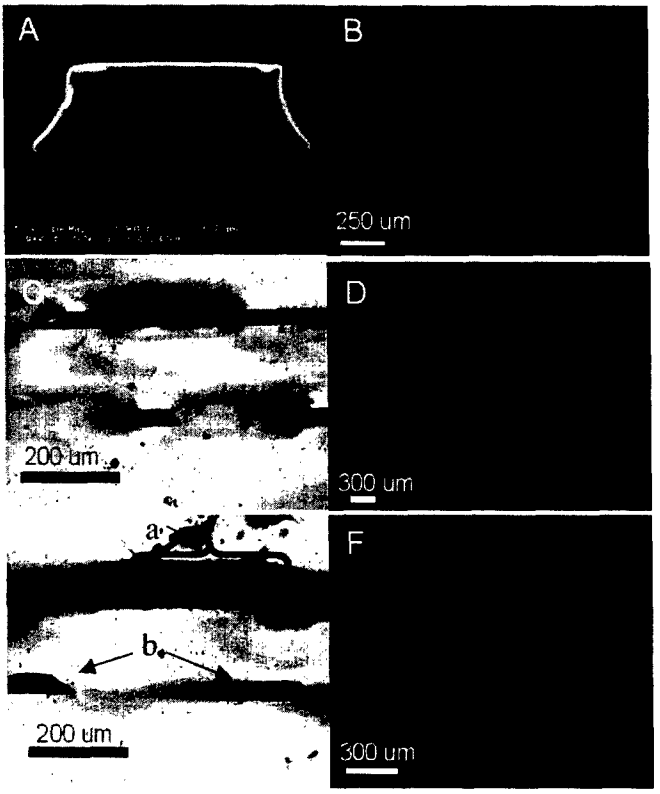

Figure 3. A) SEM cross-section of single layer PGS microfluidic channel. B) Fluorescent micrograph of rhodamine solution flowing through first generation single layer PGS microfluidic device (See Figure 1A). C) Light micrograph of cross-section of a two-layer PGS microfluidic device with vascular flow geometry. D) Fluorescent micrograph of rhodamine solution flowing through a coupled-flow two-layer PGS microfluidic device with a second-generation vascular flow geometry (See Figure 1C). E) Light micrograph of a cross-section of a two-layer PGS device containing a parenchymal layer and a vascular layer. A post from the parenchymal layer (a) is shown in close proximity to two vascular microchannels (b). F) Digitally combined fluorescent image of decoupled flow devices with DAPI solution flowing through the parenchymal microfluidic layer and rhodamine solution flowing through the vascular layer.

PGS Microfluidic Devices. Both single-layer and multi-layer PGS microfluidic devices were successfully fabricated. SEM and light micrograph cross-sections (Figure 3) supported by rhodamine flow experiments verified that the channels of both the single and multi-layer (coupled flow) devices were sealed without leakage or occlusion. Multi-layered devices with decoupled flow were also shown to successfully segregate the flow between different microfluidic layers (Figure 3F). Despite the elastic nature of PGS, there was no observable sagging throughout the microchannels within the devices. The previously outlined fabrication process was producing a very efficient device yield of approximately 90%. The trapezoidal cross-sectional geometry will be rationalized later in the discussion. The apparent skewed cross-sectional channel geometry in the mutli-layer device (Figure 3C, Figure 3E) can simply be attributed to the relative angle between the channel face and the cutting face used to make the cross-section.

Discussion

Calculation of Length Scale for Diffusion of Oxygen and Carbon Dioxide Gas in PGS Membranes. Determining the relevant transport coefficients of oxygen and carbon dioxide in PGS is a critical step in designing complex, multi-level tissue engineering systems. With this knowledge, it is important to determine the order of magnitude of the critical length scale for mass transport within PGS for designing solid supports with substantial volumes for tissue engineering applications. To study the diffusion limits of solid PGS, a mass transfer problem involving the supply of oxygen across a layer of PGS to a monolayer of mammalian cells was studied. A simple one-dimensional diffusion-reaction model can be used to determine the maximum thickness of a PGS layer that ensures adequate oxygen supply to a cell monolayer through diffusion alone. Assuming atmospheric oxygen concentrations and standard cell metabolism, the appropriate thickness was calculated by flux matching of diffusion and oxygen consumption shown respectively in the following equations:

$$J_{diff} = \frac{Perm \cdot \Delta P}{\delta}$$

$$J_{O_2,cons} = [\text{Cell Surface Density}] \bullet [\text{Consumption Rate}]$$

The results of this calculation suggest that a PGS membrane thickness (δ) of approximately 27 microns is necessary to satisfy the aforementioned conditions. Even if the most ideal conditions for transport were achieved, the fabrication of high-volume, solid PGS tissue engineering scaffolds would lead to hypoxic regions throughout the device if appropriate precautions are not taken. Therefore, all of the required oxygen for the cells within solid PGS scaffolds must be supplied via the media. To this end, hyper-oxygenated may be required to achieve sufficient concentrations within the media to supply the entire cell population within the device.

Evaluation of PGS Microfluidic Devices. The ability for PGS layers to bond via cross-linking has resulted in high strength interfaces between PGS layers. These chemical bonds are strong enough that failure of the material often occurs before delamination between the layers. This results in hermetically sealed microchannels that can handle high-pressure liquids effectively. The junction between the patterned and unpatterned layers is virtually indistinguishable in the SEM cross-section of a typical microchannel (Figure 3A)

The height of the microchannels in Figures 3A, 3C, and 3E was measured to be approximately 80% of the feature height of the microfabricated master. This effect can be attributed to the depression of the highly cross-linked PGS patterned layer into the low cross-linked PGS unpatterned layer. There is very little control in this process as there are many factors that can affect the channel height including the degree of polymerization of the semi-cured layer and the force applied when sealing the two layers together. The microchannels also have a trapezoidal cross-sectional geometry instead of the expected rectangular shape. The presence of "feet" can be attributed to a sucrose-wetting artifact during the spin coating of the sacrificial sucrose layer. Fluid mechanic simulations (data not shown) suggest the effect of this non-ideal geometry on the velocity profile is negligible when compared to flow in a hypothetical perfect rectangular channel that has been formed through ideal replica molding.

Conclusions

Single layer and multiple layer microfluidic scaffolds were successfully fabricated using PGS, a novel biocompatible and biodegradable elastomer. This work has therefore provided the groundwork for future studies in biodegradable microfluidic scaffolds using PGS. The exciting properties of this new material as well as the demonstrated capability for scale-up has shown promise for the use of this fabrication technique in a wide-variety microscale tissue engineering applications.

Acknowledgements

The authors would like to thank the contributions made by Yadong Wang of the Georgia Institute of Technology as well as Brian Orrick and the entire MEMS group at the Draper Laboratory. Funding provided by the Draper Laboratory.

References

1. **Borenstein J. T., T.H., King K. R., Weinberg E. J., Kaazempur-Mofrad M. R., Vacanti J. P. Microfabrication Technology for Vascularized Tissue Engineering.** ***Biomedical Microdevices*** **4, 167-175 (2002).**
2. **Kaihara S., B.J., Koka R., Lalan S., Ochoa E. R., Ravens M., Pien H., Cunningham B., Vacanti J. P. Silicon Micromachining to Tissue Engineer Branched Vascular Channels for Liver Fabrication.** ***Tissue Engineering*** **6, 105-117 (2000).**
3. **Wang Y., A.G.A., Sheppard B. J., Langer R. A Tough Biodegradable Elastomer.** ***Nature Biotechnology*** **20, 602-606 (2002).**
4. **Wang Y., K.Y.M., Langer R., In Vivo Degradation Characteristics of Poly(Glycerol-Sebacate).** ***Journal of Biomedical Materials Research*** **66A, 192-197 (2003).**
5. **Sok R. M. Permeation of Small Molecules across a Polymer Membrane: A Computer Simulation Study.** ***University Library Groningen*** **Dissertation, 1-129 (1994).**
6. **Duffy D. C., M.J.C., Schueller J. A., Whitesides G. M. Rapid Prototyping of Microfluidic Systems in Poly(Dimethylsiloxane).** ***Analytical Chemistry*** **70, 4974-4984 (1998).**